



HOKKAIDO UNIVERSITY

Title	Absolute configurations of (-)-hirsutanol A and (-)-hirsutanol C produced by <i>Gloeostereum incarnatum</i>
Author(s)	Asai, Ryo; Mitsuhashi, Shinya; Shigetomi, Kengo et al.
Citation	Journal of Antibiotics, 64(10), 693-696 https://doi.org/10.1038/ja.2011.73
Issue Date	2011-10
Doc URL	https://hdl.handle.net/2115/48723
Type	journal article
File Information	JoA64-10_693-696.pdf



Absolute configurations of (-)-hirsutanol A and (-)-hirsutanol C produced by *Gloeostereum incarnatum*

Ryo Asai,¹ Shinya Mitsuhashi,¹ Kengo Shigetomi,¹ Toshizumi Miyamoto,²

and Makoto Ubukata^{1*}

¹Division of Applied Bioscience, Graduate School of Agriculture, and ²Division of Environmental Resources, Hokkaido University, Kita-9, Nishi-9, Kita-ku, Sapporo 060-8589, Japan

Received :

Corresponding Author. *Tel: +81-11-706-3638. Fax: +81-11-706-3843.

E-mail: m-ub@for.agr.hokudai.ac.jp

KEYWORD: antitumor substance; *Gloeostereum incarnatum*; hirsutanol; incarnal; mushroom; sesquiterpene

INTRODUCTION

Gloeostereum incarnatum is an edible mushroom appears on broad-leaved wood in eastern Asia, northern Japan, northern China and eastern Siberia (1, 2). We have focused our attention on library construction of fungal strains of mushrooms as a screening source for the biologically active small molecules useful for forward chemical genetics and development of medicinal remedy. During the course of the screening program for potential chemopreventive agents against murine B16 melanoma cells, we found potent antiproliferative activity in a culture broth of *Gloeostereum incarnatum* HUWCB-0029 picked in the Sapporo campus of Hokkaido University, Japan. The active compound, (-)-hirsutanol A (**1**) was purified with an inactive related compound, (-)-hirsutanol C (**2**) through bioassay-guided isolation. After derivatizing **1** to (+)-incarnal (**3**), we confirmed that the strain produced trace amount of **3**, too.

In this article, we describe full details of isolation, unambiguous determination of the absolute configurations of (-)-hirsutanol A (**1**) and (-)-hirsutanol C (**2**) and their biological activities.

RESULT AND DISCUSSION

Isolation of (-)-hirsutanol A (1) and (-)-hirsutanol C (2). Bioassay-guided separation of the active compound (**1**) was achieved by the following procedures: acetone extraction of a culture of *Gloeostereum incarnatum*, EtOAc extraction, silica gel column chromatography, HPLC, and recrystallization. The most potent fraction separated by silica gel column chromatography showed two distinct peaks on HPLC (column: Xterra RP₁₈, 19 × 300 mm and solvent: 30% MeOH), and 84.6 mg of (-)-hirsutanol A (**1**) as an active compound (retention time: 65.2 min) and 76.6 mg of (-)-hirsutanol C (**2**) as an inactive compound (retention time: 83.9 min) were isolated by peak-based fraction collection.

Structure determination of (-)-hirsutanol A (1) and (-)-hirsutanol C (2). The structures of **1** and **2** deduced from FD-MS and NMR data including ¹H-¹H COSY, HMQC and HMBC, were, respectively, identical to the proposed structures of hirsutanols A and C, hirsutane-type (3) sesquiterpenes isolated from an unidentified fungus separated from an Indo-Pacific sponge *Haliclona* species (4). However, the

specific optical rotations of **1** ($[\alpha]_D^{25} = -41.9$ (c 0.97, MeOH)) and **2** ($[\alpha]_D^{25} = -8.8$ (c 0.31, MeOH)) were not identical to those of hirsutanols A ($[\alpha]_D^{25} = -23.5$ (c 0.97, MeOH)) and C ($[\alpha]_D^{25} = +20.6$ (c 0.31, MeOH)) respectively.

Fig. 1

Significant differences between the data of **2** and those of hirsutanol C (^{13}C NMR, see Table S1) make us to pursue unambiguous structure determination of both **1** and **2** (Fig. 1). First, we determined the relative configuration of **1** and **2** through differential NOE experiments and molecular modeling (5) (Fig. 1B). The NOE data are tabulated with assignments of ^1H NMR of **1** and **2** in Table S2. Observed NOEs of **1** between H-9 and 1-OH, between Me-12 and H-11 $_{\beta}$, between Me-12 and Me-14, and NOEs of **2** between H-9 and 1-OH, between Me-12 and H-11 $_{\beta}$, between H-11 $_{\beta}$ and Me-14, between H-3 and 1-OH are critical and the data assisted molecular modeling of **1** and **2**. We next determined each absolute configuration at C-9 positions of **1** and **2** to be *S* configuration by the advanced Mosher method (6) in conjunction with conformational analysis (7). (-)-Hirsutanol A (**1**) was converted into the corresponding (*S*)-MTPA ester (**1a**) and (*R*)-MTPA ester (**1b**), and (-)-hirsutanol C (**2**) was converted into the corresponding (*S*)-MTPA ester (**2a**) and (*R*)-MTPA ester (**2b**). The chemical-shift differences ($\Delta\delta = \delta_{1a} - \delta_{1b}$ and $\Delta\delta = \delta_{2a} - \delta_{2b}$) by the advanced Mosher method are shown in Fig. S1, thus **1** and **2** have the absolute configurations depicted in Fig. 1A. In addition, (-)-hirsutanol A (**1**) was converted into an oxidized compound **3** by the Dess-Martin oxidation (8) as shown in Fig. 1A. The physicochemical properties of **3** agreed well with the data including the melting point of incarnal, whose relative configuration was unambiguously determined by X-ray crystallography (9). Table S3 indicates ^{13}C NMR differences between **3** and incarnal. Although neither specific optical rotation nor circular dichroism data of incarnal was given in the literature, the authors mentioned that incarnal was isolated from culture fluid of *Gloeostereum incarnatum* (9). To confirm whether our strain (*Gloeostereum incarnatum* HUWCB-0029) produced incarnal or not, we further analyzed another active fraction on the silica gel column chromatography. We found a small peak, which shows identical UV pattern and retention time to those

of **3** on analytical HPLC with a photodiode array detector (each retention time: 9.5 min, Waters ODS, 3.9 x 150 mm, 30%-100% MeOH linear gradient, 0.8 ml/min, 40 °C). Thus absolute configuration of incarnal would be the same as that of compound **3**. Because both optical rotations of **1** and hirsutanol A, a major component from an unidentified fungus (*4*) are negative and the ¹³C NMR data of **1** is in accord with that of hirsutanol A as shown in Table S1, compound **1** is identical to hirsutanol A. On the contrary, optical rotation of **2** is opposite to that of hirsutanol C, a minor component from unidentified fungus (*4*), however the ¹³C NMR data of **2** is well matched with that of hirsutanol C except C-3 position, whose chemical shift is in the region of the solvent signals of CD₃OD. We therefore concluded that compound **2** is identical to hirsutanol C, and the sample of hirsutanol C might contain impurities, which have an influence on physicochemical properties of the compound, or some miscue analysis was done in the study of hirsutanol C isolated from the unidentified fungus (*4*).

Biological activities of (-)-hirsutanol A (1**) and (-)-hirsutanol C (**2**).**

(-)-Hirsutanol A (**1**) and (+)-incarnal (**3**) exhibited antiproliferative activity against murine B16 melanoma cells with IC₅₀ of 25 μM and 14 μM, respectively, whereas (-)-hirsutanol C (**2**) did not show activity at 200 μM as shown in Table 1. Both **1** and **2** did not show antibacterial activity against Gram-positive bacteria, *Staphylococcus aureus* and *Bacillus subtilis*, and Gram-negative bacteria, *Escherichia coli* at 100 μM, which was evaluated by a broth microdilution method based on National Committee for Clinical Laboratory Standards (NCCLS) guideline (*10*).

Table 1

In conclusion, the relative structure of **1** was unambiguously determined correlating with that of incarnal, which was determined by X-ray crystallography. Assignments of ¹H and ¹³C NMR of incarnal were unambiguously determined by HMQC and HMBC analyses. Physicochemical properties of **1** were similar to those of hirsutanol A, whose structure was given as the same as that of **1**. Although the absolute value of specific rotation, UV, IR, ¹H and ¹³C NMR data of **1** showed little differences in comparison with the reported data of hirsutanol A, and melting point of hirsutanol A was not given in the

literature (4), hirsutanol A could have the same structure with **1** in considering purity of the sample. The absolute configuration of hirsutanol A has not been determined, whereas the absolute configuration of **1** was unambiguously determined as shown in Fig. 1. The reported data of specific rotation, UV, IR, ^1H and ^{13}C NMR of hirsutanol C, whose structure was proposed to be the same as that of **2** shown in Fig. 1, were not identical to those of **2**. Therefore, we assigned very carefully the data of ^1H and ^{13}C NMR of **2** by using HMQC, HMBC, and DIF-NOE experiments. In addition to those assignments, we determined the absolute configuration of **2** by the advanced Mosher method, and concluded that the structure of **2** is depicted as shown in Fig. 1. (-)-Hirsutanol A (**1**) and (+)-incarnal (**3**) exhibited moderate antiproliferative activity against B16 melanoma cells, whereas (-)-hirsutanol C (**2**) showed no activity even at 200 μM . Therefore, **1** and **3** bearing carbonyl group conjugated with exo-methylene might be cysteine-targeting inhibitors of a functional protein related to cell proliferation (11). Antibacterial activity of hirsutanol A against *Bacillus subtilis* was mentioned without data (4), whereas we could not detect antibacterial activities of **1**, **2**, and **3** at the concentration of 100 μM . In the literature (9), incarnal exhibited antibacterial activity against *Staphylococcus aureus* and *Bacillus subtilis* by using the Mueller-Hinton agar dilution method. These differences might come from differences of assay method and bacterial strains. Both **1** and **3** having carbonyl moiety conjugated with exo-methylene could have weak antibacterial activities at sub-millimolar concentrations (12). Recently X-ray crystal structure of hirsutanol A isolated from the marine fungus *Chondrostereum* sp. (13) and its biological activities (14) were reported. The relative configuration of hirsutanol A and its conformation correspond to the molecular model of **1** (Fig. 1B), and specific rotation of this sample is approximately consistent with that of **1**.

EXPERIMENTAL SECTION

Materials. Fungal mycelium of *Gloeostereum incarnatum* (Japanese name: Nikawaurokotake) was collected in the Sapporo Campus of Hokkaido University, Japan.

DNA sequencing of isolate. Mycelia of isolated strain were maintained with a malt extract agar (2% malt extract and 1.5% agar) plate in a dark place at 22-24 °C. Total DNA was extracted from a block of mycelia (3 mm × 3 mm × 3 mm) using Isoplant II DNA extraction kit (Wako Pure Chemical Industries Ltd., Osaka, Japan) according to the manufacturer's instructions. The extracted DNA was dissolved in 50 µl TE buffer, and 1 µl of the DNA solution was used as template DNA. The primer pair of ribosomal DNA, ITS1f; 5'-CTT GGT CAT TTA GAG GAA GTA A-3' (sense) and ITS4; 5'-TCC TCC GCT TAT TGA TAT GC-3' (antisense), was used for PCR amplification (15, 16). The sequence of the ITS1-5.8S rDNA-ITS2 region was determined by using an ABI Auto Sequencer 3730 (Applied Biosystems, Foster City, CA). The aligned sequence well accorded with *Gloeostereum incarnatum* 3332 (BLAST Locus No. AF141637) with 98% (350/355) of identities and 0% (3/335) of gaps in a BLAST search (17).

Fermentation procedure of the producing strain. Each block (10 mm × 10 mm × 3 mm) cut off from mycelial pellet of *Gloeostereum incarnatum* spread on a malt extract agar plate was inoculated into 20 of 500-ml K-1 flasks (K-Techno, Japan) each containing 150 ml of production medium consisting of 1% malt extract, 0.5% yeast extract, and 0.5% glucose. Fermentation was carried out in a dark place at 25 °C for 30 days in stationary culture.

General Experimental Procedures for Structural Study. Unless otherwise stated, chemicals of the highest commercial purity were used without further purification. The melting point was measured by a Mettler Melting-Point Apparatus FP-5 for (-)-hirsutanol A (**1**) and (-)-hirsutanol C (**2**), and a Yanagimoto Micro-Melting Point Apparatus for (+)-incarnal (**3**). UV spectra of **1**, **2** and **3** were recorded on a HITACHI L7455 photodiode array detector at 30 °C; IR spectra were recorded on a Digilab FTS-50A; ¹H, ¹³C, HH-COSY, HMBC, HMQC, DIF-NOE and NOESY NMR spectra were measured with a Bruker AMX-500 (500 MHz) or JEOL JNM-EX270 (270 MHz). Chemical shifts are reported in δ ppm using tetramethylsilane as internal standard, and coupling constants (*J*) are given in Hertz. Mass spectra were acquired with FD techniques using a JMS-SX102A. A part of the NMR and MS spectra were measured at the GC-MS and NMR Laboratory, Faculty of Agriculture, Hokkaido University. Optical rotations were determined on a JASCO P-2200 polarimeter in 3.4 mm × 5.0 cm cells at 25 °C.

Extraction and Isolation. Acetone of 300 ml was added to each culture, after cutting mycelial pellet into small pieces with scissors, the combined resultant suspension was stirred overnight at 4 °C and filtered with Büchner funnel (filter paper, ADVANTEC No3) under reduced pressure. The filtrate was evaporated *in vacuo*, and the aqueous solution was extracted twice with equal part of ethyl acetate. The combined organic layer was evaporated *in vacuo* to give a crude extract. The extract was subjected to silica gel column chromatography by stepwise elution with the following solvent systems; CHCl₃ : MeOH = 25 : 1, 9 : 1, 4 : 1, and 0 : 1 to give 17 fractions. The fraction nine showed most potent antiproliferative activity was purified by HPLC (pump: Waters 600, column: Xterra RP₁₈, 7µm, 19 x 300 mm, solvent: 30% MeOH) to give 84.6 mg of **1** and 76.6 mg of **2**. The fraction three showed antiproliferative activity showed similar R_f value (*R_f* 0.57-0.85) to that of synthetic **3** (*R_f* 0.65) on the silica gel TLC (EtOAc : hexane, 4 : 1). The fraction showed a small peak having the identical UV pattern and retention time (9.5 min) to those of **3** on HPLC with a photodiode array detector (Waters Nova-Pak C18, 3.9 x 150 mm, 30%-100% MeOH linear gradient, 0.8 ml/min, 40 °C).

(-)-Hirsutanol A (**1**), mp 149-150 °C [lit., 161-163 °C (*13*)]. $[\alpha]_D^{25} = -41.9$ (*c* 0.97, CH₃OH) [lit., hirsutanol A: $[\alpha]_D^{25} = -23.5$ (*c* 0.97, CH₃OH) (*4*); $[\alpha]_D^{20} = -52.4$ (*c* 0.21, CH₃OH) (*13*)]. UV(200-400 nm (AU)): 309 (2.41), 217 (1.62). ¹H NMR (270 MHz, CDCl₃) 0.99 (3H, s, H-14), 1.27 (3H, s, H-12), 1.34 (3H, s, H-15), 1.79 (1H, d, *J* = 14.8 Hz, H-11α), 2.25 (1H, d, *J* = 14.8 Hz, 11β), 4.71 (1H, d, *J* = 6.9, 2.3 Hz, H-9), 5.24 (1H, s, H-13a), 6.10 (2H, H-5 and 13b, overlapping), 6.51 (1H, d, *J* = 2.3 Hz, H-7); (270 MHz, CD₃OD, see Figure S2) 0.95 (3H, H-14), 1.23 (3H, s, H-12), 1.29 (3H, s, H-15), 1.70 (1H, d, *J* = 14.9 Hz, H-11α), 2.27 (1H, d, *J* = 14.8 Hz, H-11β; the chemical shift, 2.67 ppm in ref. 4 may be typographical error), 4.63 (1H, d, *J* = 2.3 Hz, H-9), 5.27 (1H, s, H-13a), 5.96 (1H, s, H-13b; 6.00 ppm is assigned to H-13b in ref. 4), 6.02 (1H, s, H-5), 6.50 (1H, d, *J* = 2.4 Hz, H-7); (270 MHz, DMSO-*d*₆): See Table 2S. ¹³C NMR (67.5 Hz, CD₃OD): See Table 1S and Figure S3. FD (*m/z*):

246(100) $[M]^+$, 228(25) $[M-H_2O]^+$, 218(75) $[M-CO]^+$. FD-HRMS m/z $[M]^+$ calcd for $C_{15}H_{18}O_3$, 246.12559; found, 246.12595.

(-)-Hirsutanol C (**2**), mp 205-206 °C. $[\alpha]_D^{25} = -8.8$ (c 0.31, CH_3OH) [lit., hirsutanol C: $[\alpha]_D^{25} = +20.6$ (c 0.31, CH_3OH) (4)]. UV(200-400nm (AU)): 288 (2.01), 206 (0.44, sh). 1H NMR (270 MHz, $CDCl_3$): 0.97 (3H, s, H-14), 1.04 (3H, s, H-12), 1.12 (3H, d, $J = 7.2$ Hz, H-13), 1.34 (3H, s, H-15), 1.67 (1H, d, $J = 14.9$ Hz, H-11 α), 2.11 (1H, d, $J = 14.9$ Hz, H-11 β), 2.86 (1H, q, $J = 7.2$ Hz, H-3), 4.73 (1H, dd, $J = 7.5, 2.4$ Hz, H-9), 5.87 (1H, s, H-5), 6.46 (1H, d, $J = 2.4$ Hz, H-7); (270 Hz, CD_3OD , see Figure S4) 0.92 (3H, s, H-14), 1.02 (3H, s, H-12), 1.06 (3H, d, $J = 7.2$ Hz, H-13), 1.28 (3H, s, H-15), 1.60 (1H, d, $J = 14.8$ Hz, H-11 α), 2.10 (1H, d, $J = 14.8$ Hz, H-11 β), 2.89 (1H, q, $J = 7.2$ Hz, H-3), 4.65 (1H, d, $J = 2.3$ Hz, H-9), 5.76 (1H, s, H-5), 6.44 (1H, d, $J = 2.4$ Hz, H-7); (270 Hz, $DMSO-d_6$): See Table 2S. ^{13}C NMR (67.5 Hz, CD_3OD): See Table 1S and Figure S5. FDMS (m/z): 248(100) $[M]^+$, 230(26) $[M-H_2O]^+$. FD-HRMS m/z $[M]^+$ calcd for $C_{15}H_{20}O_3$, 248.14124; found, 248.14032.

(+)-Incarnal (**3**), mp 132-133 °C [lit., mp 132-133 °C (9)]. $[\alpha]_D^{25} = +339.8$ (c 0.30, CH_3OH). UV(200-400nm (AU)): 309, 217 [lit., 306, 218 (9)]. 1H NMR (270 MHz, $CDCl_3$, see Figure S6): 1.22 (3H, s, H-14), 1.28 (3H, s, H-12), 1.41 (3H, s, H-15), 1.73 (1H, s, OH-1), 2.06 (1H, d, $J = 13.9$ Hz, H-11 α), 2.26 (1H, d, $J = 13.9$ Hz, H-11 β), 5.40 (1H, s, H-13a), 6.21 (1H, s, H-13b), 6.43 (1H, s, H-5), 7.20 (1H, s, H-7). ^{13}C NMR (67.5 MHz, $CDCl_3$): see Table 3S and Figure S7. FD-HRMS m/z $[M]^+$ calcd for $C_{15}H_{16}O_3$, 244.1099; found, 244.1077.

Computational Procedure. The equilibrium geometries of all compounds were optimized by molecular mechanics (Allinger's MM2) calculations by using Spartan Student (Ver. 3.0.2, Wavefunction, Inc.). Stable conformers were confirmed by CONFLEX calculations using CAChe 4.5 for Power Macintosh (Fujitsu Ltd.) and well corresponded to the three dimensional structures of incarnal (9) and hirsutanol A (13) determined by X-ray crystallography.

Antiproliferative Assay. Murine B16 melanoma cells, which derived from C57BL/6 mouse, were maintained in Dulbecco's modified Eagle's medium containing 10% fetal bovine serum, 1.9 g/l sodium

bicarbonate, 100 µg/ml streptomycin, and 20 U/ml penicillin G at 37 °C under 5% CO₂. Antiproliferative activities were measured by Cell Counting Kit-8 (Dojindo; Tokyo, Japan). Cell Counting Kit-8 allows colorimetric assays using WST-8 [2-(2-methoxy-4-nitrophenyl)-3-(4-nitrophenyl)-5-(2,4-disulfophenyl)-2H-tetrazolium, monosodium salt], which produces a water-soluble formazan dye upon reduction in the presence of an electron carrier, 1-Methoxy PMS. WST-8 is reduced by cellular dehydrogenase to an orange formazan product that is soluble in cell culture medium. The amount of formazan produced is directly proportional to the number of living cells (18).

The B16 cells (1.0×10^4 cells/95 µl/well) were seeded into 96-well microplates, and then 5 µl of test sample was added to each well. After incubating for 24 h, 10 µl of WST-8 solution (Cell Counting Kit-8) was added to each well. After a further 1-3 h in culture, the optical density of the water-soluble formazan produced by the cells was measured with a microplate reader (Sunrise Remote, TECAN, USA) at 450 nm (reference: 595 nm). The test compound was dissolved in dimethylsulfoxide (DMSO), and the final concentration of DMSO in the medium was 1%. The IC₅₀ values were determined graphically.

Antibacterial Assay. Antibacterial activities were evaluated based on the Clinical Laboratory Standards Institute (CLSI - formerly NCCLS) guideline (10). *Staphylococcus aureus* (ATCC 6538), *Bacillus subtilis* (ATCC 70385), and *Escherichia coli* (ATCC 8739) were subjected to bioassay. Procedure of determination of antibacterial activities was performed as previously described with a slight modification (12). Briefly, assay was performed using Mueller-Hinton (MH) liquid medium containing 0.3% meat extract, 1.75% Bacto™ Peptone, and 0.15% soluble starch. After pre-culture with MH liquid medium, 5 µl of test compound solutions and 95 µl of bacterial inoculums were mixed to 5.0×10^5 colony-forming unit (CFU)/ml in 96-well microtiter plates. The plates were covered with sterile sealer and incubated at 600 rpm, 35 °C for 16 h. Bacterial growth was evaluated by measuring OD₅₉₅ value. Assays were carried out in triplicate.

ACKNOWLEDGMENT This work was partially supported by a research grant donated by the Institute for Fermentation, Osaka (IFO), Japan.

LITERATURE CITED

- (1) Imai, S. Gloeostereae S. Ito et Imai, a new tribe of Thelephoraceae. *Transaction of the Sapporo Natural History Society* **1933**, *13*, 9-11.
- (2) Petersen, R. H.; Paramasto, E. A redescription of *Gloeostereum incarnatum*. *Mycol. Res.* **1993**, *97*, 1213-1216.
- (3) Turner, W. B. ; Aldridge, D. C. Fungal Metabolites II, Academic Press: New York, 1983, 246-247.
- (4) Wang, G.-Y.-S.; Abrell, L. M.; Avelar, A.; Borgeson, B. M.; Crews, P. New hirsutane based sesquiterpenes from salt water cultures of a marine sponge-derived fungus and the terrestrial fungus *Coriolus consors*. *Tetrahedron* **1998**, *54*, 7335-7342.
- (5) Ubukata, M.; Koshino, H.; Osada, H.; Isono, K. Absolute configuration of reveromycin A, an inhibitor of the signal transduction of epidermal growth factor. *J. Chem. Soc. Chem. Commun.*, **1994**, 1877-1878.
- (6) Ohtani, I.; Kusumi, T. Kashman, T.; Kakisawa, H. High-field FT NMR application of Mosher's method. The absolute configuration of marine terpenoids. *J. Am. Chem. Soc.*, **1991**, *113*, 4-92-4096.
- (7) Ubukata, M.; Cheng, X.-C.; Isobe, M.; Isono, K. Absolute configuration of tautomycin, a protein phosphatase inhibitor from a streptomycetes. *J. Chem. Soc. Perkin Trans 1*, **1993**, 617-624.
- (8) Dess, D. B.; Martin, J. C. A useful 12-I-5 triacetoxiypoxidation (the Dess-Martin periodinate) for the selective oxidation of primary or secondary alcohols and a variety of related 12-I-5 species. *J. Am. Chem. Soc.* **1991**, *113*, 7277-7287.
- (9) Takazawa, H.; Kashino, S. Incarnal. A new antibacterial sesquiterpene from basidiomycetes. *Chem. Pharm. Bull.* **1991**, *39*, 555-557.
- (10) *Performance Standards for Antimicrobial Disk Susceptibility Tests*, 5th ed. M2-A5. 1993. Clinical

Laboratory Standards Institute (CLSI), Villanova, PA.

- (11) Ueda, K.; Usui, T.; Nakayama, H.; Ueki, M.; Takio, K.; Ubukata, M.; Osada, H. 4-Isoavenaciolide covalently binds and inhibits VHR, a dual-specific phosphatase. *FEBS Lett.* **2002**, *525*, 48-52.
- (12) Shigetomi, K.; Shoji, K.; Mitsuhashi, S.; Ubukata, M. The antibacterial properties of 5-tuliposide B. Synthesis of 6-tuliposide B analogues and structure-activity relationship. *Phytochemistry* **2010**, *71*, 312-324.
- (13) Li, H.-J.; Lan, W. -J.; Lam, C.-K.; Yang, F.; Zhu, X.-F. Hirsutane sesquiterpenoids from the marine-derived fungus *Chondrostereum* sp. *Chem. Biodivers.* **2011**, *8*, 317-324.
- (14) Yang, F.; Gao, Y.-H.; Wu, K.-W.; Deng, R.; Li, D.-D.; Wei, Z.-X.; Jiang, S.; Wu, X.-Q.; Feng, G.-K.; Li, H.-J.; Zhu, X.-F. A novel sesquiterpene hirsutanol A induces autophagical cell death in human hepatocellular carcinoma cells by increasing reactive oxygen species. *Chin. J. Cancer* **2010**, *29*, 655-660
- (15) Gardes, M.; Bruns T. D. ITS primers with enhanced specificity for basidiomycetes: application to the identification of mycorrhizae and rusts. *Molecular Ecology* **1993**, *2*, 113-118.
- (16) White T. J.; Bruns, T.; Lee, S.; Taylor J. Amplification and direct sequencing of fungal ribosomal RNA genes for phylogenics. In: PCR Protocols: a guide to methods and applications. Innis M. A.; Gelfand D. H.; Sninsky J. J.; White T. J. (eds). Academic Press: San Diego, 1990; pp 315-322.
- (17) Altschul, S. F.; Modden, T. L.; Schaffer, A. A.; Zhang, J.; Zhang, Z.; Miller W.; Lipman, D. J. Gapped BLAST and PSI-BLAST: a new generation of protein database search program. *Nucleic Acids Res.* **1997**, *25*, 3389-3402.
- (18) Matsuda, H.; Nakashima, S.; Oda, Y.; Nakamura, S.; Yoshikawa, M. Melanogenesis inhibitors from the rhizomes of *Alpinia officinarum* in B16 melanoma cells. *Bioorg. Med. Chem.* **2009**, *17*,

6048-6053.

Supplementary Information accompanies the paper on The Journal of Antibiotics website.

Table 1. Biological activities of (-)-hirsutanol A (**1**), (-)-hirsutanol C (**2**), and (+)-incarnal (**3**).

Test organism		Compound			
		1	2	3	incarnal ^a
B16 melanoma cells	[IC ₅₀ (μM)]	25.6	>200	14.4	ND ^b
<i>Staphylococcus aureus</i>	[MIC(μM)]	>100	>100	>100	25.6 ^c
<i>Bacillus subtilis</i>	[MIC(μM)]	>100	>100	>100	51.2 ^c
<i>Escherichia coli</i>	[MIC(μM)]	>100	>100	>100	>400 ^c

^a Biological activities reported in ref. 9. ^b Not determined. ^c Mueller-Hinton agar dilution method.

Figure Captions.

Fig. 1. The stereochemistry of (-)-hirsutanol A (**1**), (-)-hirsutanol C (**2**), and (+)-incarnal (**3**). (A) Absolute configurations of **1** and **2**, and conversion of **1** into **3** by the Dess-Martin oxidation. (B) Stable conformers of **1** and **2** based on the MM2 force field calculation. Numbering corresponds to Table S2. The predicted minimum interproton distances support the interpretation of NOE results (see text).

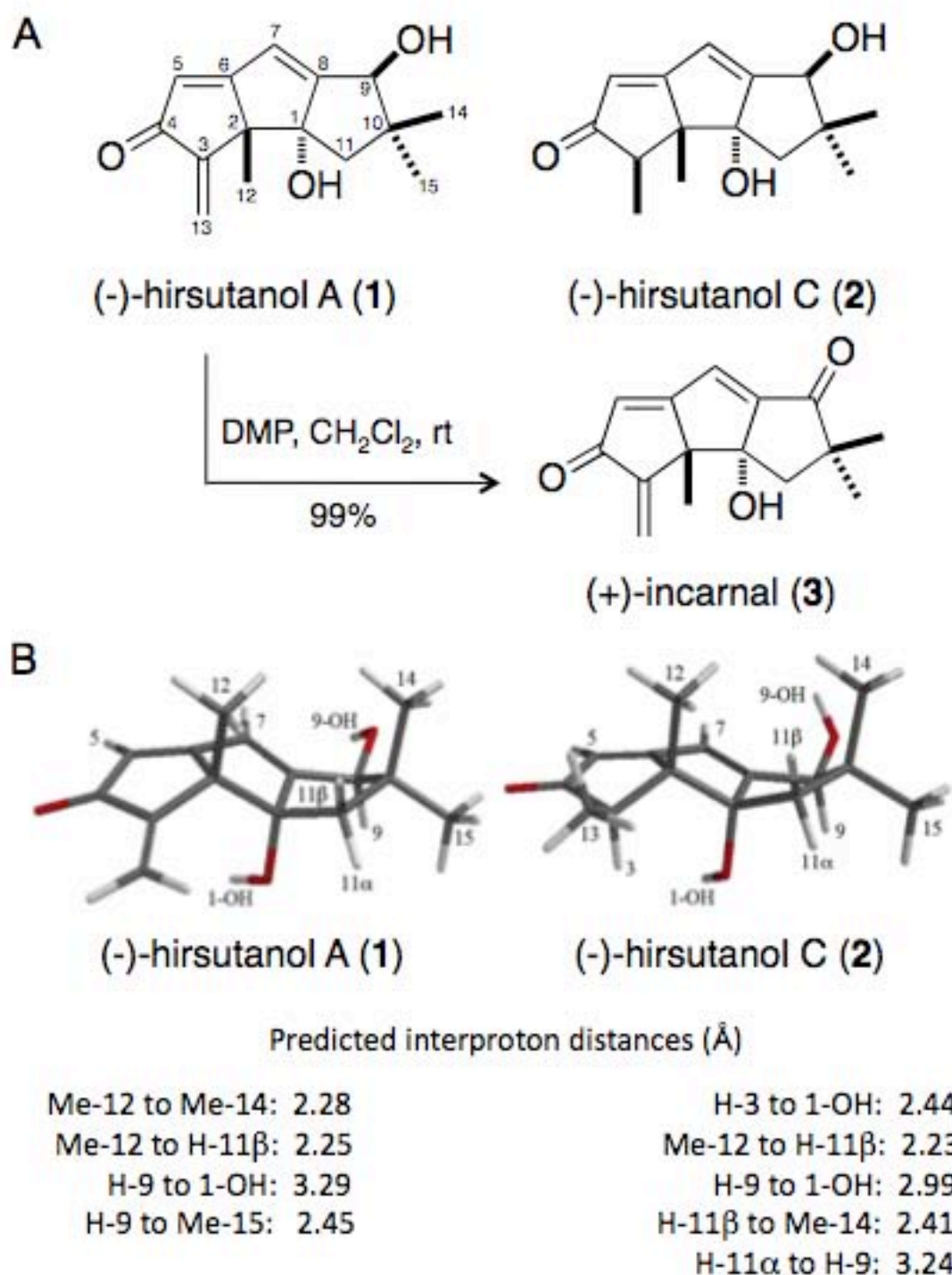


Fig. 1